Solution of the Amati-Bertocchi-Fubini-Stanghellini-Tonin Equation with a Resonance Kernel*

C. F. Chan and B. R. Webber†
Lawrence Berkeley Laboratory, University of California, Berkeley, California 94720
(Received 1 November 1971)

The solution of the Amati-Bertocchi-Fubini-Stanghellini-Tonin multiperipheral integral equation with a narrow-resonance kernel is investigated. First, an approximation scheme that leads to a tractable analytic approximate solution is presented for both the forward and nonforward equations. Next, the exact numerical solutions are displayed for the relevant values of the input parameters: These results serve as a measure of the accuracy of various analytic approximate solutions. The approximate solution presented here, which is found to be good to within about 10% in the region of interest, should be useful both in the general study of the output of the multiperipheral model and in the Pomeranchukon perturbation theory.

I. INTRODUCTION

In this paper we shall investigate in two complementary ways the solution of the Amati-Bertocchi-Fubini-Stanghellini-Tonin (ABFST) multiperipheral integral equation,[1] in the modern version formulated by Chew, Rogers, and Snider,[2] and by Abarbanel, Chew, Goldberger, and Saunders.[3] We shall study in detail the solution of the equation with the simplest kernel consisting of a single sharp resonance, and discuss only briefly the straightforward generalization to the case of a kernel with many resonances. This solution, in the language of Ref. 3, corresponds to the "unperturbed solution," since we neglect the small high-subenergy diffractive-scattering part in the input kernel.

In order to gain insight into the nature of the output, we first obtain an analytic approximate solution by replacing the original kernel by a factorizable kernel. This replacement is guided in some sense by "peripheralism," that is, the factorizable kernel should behave like the original kernel in the peripheral region, where the contribution to any convergent integral involved is expected to be important. We shall demonstrate that the solution so obtained reproduces itself under the action of the original kernel in the most peripheral region.

On the other hand, we have also solved the equation numerically for certain values of the input parameters. This solution provides a measure of the accuracy of various analytic approximate solutions.

Our analytic approximate method is presented in Sec. II (for forward scattering) and Sec. III (for nonforward scattering). There is no pretense of rigor; rather, in a practical way we shall develop a tractable explicit form that is simple enough and yet has reasonable accuracy. The latter point is justified by comparing with the exact numerical solution which is presented in Sec. IV. Some generalizations and the question of the uniqueness of our approximation scheme are presented at the end of the paper.

II. THE FORWARD EQUATION AND THE APPROXIMATE SOLUTION

We shall first illustrate the properties of our approximation in the case of forward scattering ($q = 0$ in Fig. 1). Let us here ignore the problem of internal symmetry; this can easily be incorporated into the model by introducing crossing matrices as described in Ref. 3. The absorptive part A of the elastic amplitude T of pseudoscalar-meson–pseudoscalar-meson scattering is normalized in such a way that

$$A(s, \mu^2, \mu^2) = \Delta^{1/2}(s, \mu^2, \mu^2)\sigma^{\mathrm{tot}}(s, \mu^2, \mu^2), \tag{2.1}$$

where μ^2 is the meson mass squared,

$$\Delta(x, y, z) = x^2 + y^2 + z^2 - 2(xy + yz + zx),$$

and σ^{tot} is the total meson-meson (μ-μ) cross section. The elastic μ-μ cross section σ^{el} enters in the input potential of the equation in the (on-shell) form

$$V(s, \mu^2, \mu^2) = \Delta^{1/2}(s, \mu^2, \mu^2)\sigma^{\mathrm{el}}(s, \mu^2, \mu^2). \tag{2.2}$$

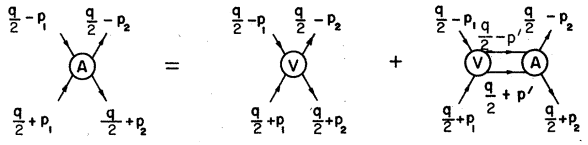

FIG. 1. The kinematic structure of the multiperipheral integral equation.

TABLE I. The variables.

$s=(p_1-p_2)^2$	$\cosh\theta=\dfrac{-p_1\cdot p_2}{(-\tau_1)^{1/2}(-\tau_2)^{1/2}}=\dfrac{s-\tau_1-\tau_2}{2(-\tau_1)^{1/2}(-\tau_2)^{1/2}}$
$t=q^2$	
$\tau_1=p_1{}^2$	$z_1=\dfrac{p_1\cdot q}{(-\tau_1)^{1/2}(-t)^{1/2}}$
$\tau_2=p_2{}^2$	$z_2=\dfrac{p_2\cdot q}{(-\tau_2)^{1/2}(-t)^{1/2}}$
$\tau'=p'^2$	$z'=\dfrac{p'\cdot q}{(-\tau')^{1/2}(-t)^{1/2}}$
	$-1\le z\le 1$ for all z's
	$\cosh\psi=\dfrac{\cosh\theta-z_1z_2}{(1-z_1{}^2)^{1/2}(1-z_2{}^2)^{1/2}}$

The O(1, 3) partial wave of A is defined as (cf. Table I)

$$A_\lambda(\tau_1,\tau_2)=\int_{4\mu^2}^{\infty} ds\, e^{-(\lambda+1)\theta(s,\tau_1,\tau_2)}A(s,\tau_1,\tau_2); \tag{2.3}$$

the inverse transform is

$$A(s,\tau_1,\tau_2)=\int_{c-i\infty}^{c+i\infty}\frac{d\lambda}{2\pi i}\,\frac{e^{+(\lambda+1)\theta(s,\tau_1,\tau_2)}}{2(-\tau_1)^{1/2}(-\tau_2)^{1/2}\sinh\theta(s,\tau_1,\tau_2)}A_\lambda(\tau_1,\tau_2), \tag{2.4}$$

where the contour is taken to the right of any singularity of A_λ in the λ plane. In terms of A_λ, the ABFST equation is

$$A_\lambda(\tau_1,\tau_2)=V_\lambda(\tau_1,\tau_2)+\frac{1}{16\pi^3(\lambda+1)}\int_{-\infty}^{0}\frac{d\tau'}{(\mu^2-\tau')^2}V_\lambda(\tau_1,\tau')A_\lambda(\tau',\tau_2). \tag{2.5}$$

The essence of our method is to approximate

$$e^{-\theta(s,\tau_1,\tau_2)}=\frac{2(-\tau_1)^{1/2}(-\tau_2)^{1/2}}{(s-\tau_1-\tau_2)+[(s-\tau_1-\tau_2)^2-4(-\tau_1)(-\tau_2)]^{1/2}} \tag{2.6}$$

by a factorizable expression[4]

$$\xi(s,\tau_1,\tau_2)\equiv\frac{(-s\tau_1)^{1/2}(-s\tau_2)^{1/2}}{(s-\tau_1)(s-\tau_2)}. \tag{2.7}$$

The function ξ is actually a lower bound to $e^{-\theta}$. Notice that

$$e^{-\theta(s,\tau_1,\tau_2)}\sim\xi(s,\tau_1,\tau_2)[1+2(-\tau_1)(-\tau_2)/s^2] \tag{2.8}$$

when either τ_1 or τ_2, or both, approach zero. When either τ_1 or τ_2, or both, approach (minus) infinity, the two expressions are different. One hopes that, in any convergent integral involved in the calculation, the contributions from these "nonperipheral" regions do not matter very much. Notice also that ξ is a small quantity for all values of τ_1 and τ_2. For a given s, it has an absolute maximum

$$\xi(s,\tau_1,\tau_2)\Big|^{\text{abs max}}_{\tau_1=\tau_2=-s}=\tfrac{1}{4}, \tag{2.9}$$

whereas

$$e^{-\theta(s,\tau_1,\tau_2)}\Big|^{\max}_{\text{fixed }\tau_2,\,-\tau_1=s-\tau_2}=\frac{(s-\tau_2)^{1/2}-(s)^{1/2}}{(-\tau_2)^{1/2}}\le 1,$$

approaching the absolute maximum value of 1 for $-\tau_1=-\tau_2\gg s$.

With this approximation, Eq. (2.5) is immediately soluble. Here we consider the solution for the kernel with a single (sharp) resonance. A kernel with many resonances will be discussed in Sec. V. Thus we put for the (on-shell) potential

$$V(s,\mu^2,\mu^2)=\Delta^{1/2}(s,\mu^2,\mu^2)\pi mx\Gamma\sigma^{\text{el}}_{\max}\delta(s-m^2)\equiv m^2R(0)\delta(s-m^2), \tag{2.10}$$

where m^2, x, and Γ are the squared mass, elasticity, and width of the μ-μ resonance. We shall assume $\mu^2\ll m^2$. The solution to Eq. (2.5) is then

$$A_\lambda(\tau_1,\tau_2)=\frac{m^2R(0)}{1-\mathrm{Tr}K_\lambda}\left(\frac{(-m^2\tau_1)^{1/2}(-m^2\tau_2)^{1/2}}{(m^2-\tau_1)(m^2-\tau_2)}\right)^{\lambda+1}, \tag{2.11}$$

where

$$\mathrm{Tr}K_\lambda = \frac{m^2 R(0)}{16\pi^3(\lambda+1)} \int_{-\infty}^{0} \frac{d\tau}{(\mu^2-\tau)^2} \left(\frac{-m^2\tau}{(m^2-\tau)^2}\right)^{\lambda+1} \tag{2.12}$$

$$= \frac{R(0)}{16\pi^3} B(\lambda+2, \lambda+2) F(2, \lambda+2, 2\lambda+4, 1-\mu^2/m^2) \tag{2.13}$$

$$= \frac{R(0)}{16\pi^3} \frac{B(\lambda,\lambda)}{2(2\lambda+1)} \quad \text{for } \mu^2 = 0. \tag{2.14}$$

In Eqs. (2.13) and (2.14), B is the Euler beta function and F is the hypergeometric function. The eigenvalue condition is given by the vanishing of the Fredholm determinant

$$D(\lambda) = 1 - \mathrm{Tr}K_\lambda = 0. \tag{2.15}$$

A special property of this approximate solution is that, under the action of the original kernel, it "reproduces itself" for $-\tau_1$, $-\tau_2$, or both, small (in comparison with m^2). This can best be illustrated by going back to the s plane. From Eqs. (2.4) and (2.11), we get for the leading behavior of the full amplitude

$$A(s, \tau_1, \tau_2) \underset{s\to\infty}{\sim} 16\pi^3 \beta_\alpha \left(\frac{m^2}{m^2-\tau_1}\right)^{\alpha+1} \left(\frac{m^2}{m^2-\tau_2}\right)^{\alpha+1} \left(\frac{s}{m^2}\right)^{\alpha}, \tag{2.16}$$

where α is the largest value of λ satisfying Eq. (2.15), and

$$\beta_\alpha = -\left(\frac{\partial}{\partial\lambda} \frac{16\pi^3}{R(0)} \mathrm{Tr}K_\lambda\right)^{-1}_{\lambda=\alpha}. \tag{2.17}$$

In the interest of simplicity and clarity, let us put $\mu^2 = 0$ for the moment; then the amplitude at the physical (and most peripheral) point is

$$A(s, 0, 0) \underset{s\to\infty}{\sim} 16\pi^3 \beta_\alpha (s/m^2)^\alpha. \tag{2.18}$$

On the other hand, in this asymptotic region of the s plane, the full amplitude, when written in the form

$$A(s, \tau_1, \tau_2) \underset{s\to\infty}{\sim} \phi_\alpha(\tau_1, \tau_2) s^\alpha, \tag{2.19}$$

satisfies an equation corresponding to Eq. (2.5):

$$[(-\tau_1)^{1/2}(-\tau_2)^{1/2}]^{\alpha+1} \phi_\alpha(\tau_1, \tau_2) \sim \frac{1}{16\pi^3(\alpha+1)} \int ds\, V(s, \tau_1, \tau') \int_{-\infty}^{0} \frac{d\tau'}{(\mu^2-\tau')^2} e^{-(\alpha+1)\theta(s,\tau_1,\tau')} \times [(-\tau')^{1/2}(-\tau_2)^{1/2}]^{\alpha+1} \phi_\alpha(\tau', \tau_2). \tag{2.20}$$

If we put Eq. (2.16) as a trial function into the right-hand side of Eq. (2.20) with the original kernel, the *output* physical amplitude is

$$A(s, 0, 0) \sim \lim_{\tau_1, \tau_2 \to 0} \phi_\alpha(\tau_1, \tau_2) s^\alpha \tag{2.21}$$

$$\sim \frac{m^2 R(0)}{16\pi^3(\alpha+1)} \int_{-\infty}^{0} \frac{d\tau'}{\tau'^2} \left(\frac{-\tau'}{m^2-\tau'}\right)^{\alpha+1} 16\pi^3 \beta_\alpha \left(\frac{m^2}{m^2-\tau'}\right)^{\alpha+1} \left(\frac{s}{m^2}\right)^{\alpha}, \tag{2.22}$$

which is just Eq. (2.18) by virtue of Eqs. (2.12) and (2.15). (Actually the condition $\tau_2 = 0$ is not necessary in this part of the argument; τ_2 can take any value.) The corresponding property can of course be demonstrated in the λ plane. It should be noted that some previously proposed approximate solutions [5-8] do not possess this property. Comparisons of the solution proposed here and other approximate solutions with the exact numerical solution will be given in Sec. IV.

III. THE NONFORWARD EQUATION AND ITS APPROXIMATE SOLUTION

Away from $t = 0$, the on-shell potential is given by

$$V(s, t) = \frac{1}{16\pi^2 \Delta^{1/2}(s, \mu^2, \mu^2)} \int \frac{dt_1\, dt_2\, \theta(-\Delta(t, t_1, t_2) + 4tt_1t_2/(s-4\mu^2))}{[-\Delta(t, t_1, t_2) + 4tt_1t_2/(s-4\mu^2)]^{1/2}} T^*(s, t_1) T(s, t_2), \tag{3.1}$$

where T is the complete elastic amplitude; $\mathrm{Im}T(s, t) = A(s, t)$.

A single (sharp) resonance contributes a potential

$$V(s,t)=2\times\frac{16\pi s}{\Delta^{1/2}(s,\mu^2,\mu^2)}(2L+1)P_L(z_s)\pi mx\Gamma\delta(s-m^2)$$
$$\equiv m^2R(t)\delta(s-m^2), \tag{3.2}$$

where

$$z_s=1+\frac{2s}{\Delta(s,\mu^2,\mu^2)}t$$

and L is the spin of the resonance.

The appropriate O(1, 2) partial-wave amplitude is

$$A_l(\tau_1,z_1,\tau_2,z_2;t)=\int_{4\mu^2}^{\infty}ds\,Q_l(\cosh\psi)A(\psi,\tau_1,z_1,\tau_2,z_2;t), \tag{3.3}$$

and the inverse transform is

$$A(\psi,\tau_1,z_1,\tau_2,z_2;t)=\int_{c-i\infty}^{c+i\infty}\frac{dl}{2\pi i}\frac{(2l+1)P_l(\cosh\psi)}{2[(-\tau_1)(1-z_1^2)(-\tau_2)(1-z_2^2)]^{1/2}}A_l(\tau_1,z_1,\tau_2,z_2;t), \tag{3.4}$$

where the contour is taken to the right of any singularity of A_l in the l plane.

In terms of A_l, the nonforward ABFST equation is

$$A_l(\tau_1,z_1,\tau_2,z_2;t)=V_l(\tau_1,z_1,\tau_2,z_2;t)+\frac{1}{16\pi^4}\int_{-\infty}^{0}d\tau'\int_{-1}^{+1}\frac{dz'(1-z'^2)^{-1/2}}{(\mu^2-\tau'-\frac{1}{4}t)^2-\tau' tz'^2}V_l(\tau_1,z_1,\tau',z';t)$$
$$\times A_l(\tau',z',\tau_2,z_2;t). \tag{3.5}$$

In order to make an approximation similar to that discussed in Sec. II, we note that the function $Q_l(\cosh\psi)$ can be expanded as[9]

$$Q_l(\cosh\psi)=\sum_{n=0}^{\infty}\frac{\Gamma^2(l+1)2^{2l+1}n!}{\Gamma(2l+2+n)}[(1-z_1^2)^{(l+1)/2}C_n^{l+1}(z_1)][(1-z_2^2)^{(l+1)/2}C_n^{l+1}(z_2)]e^{-(l+1+n)\theta(s,\tau_1,\tau_2)}, \tag{3.6}$$

where C_n^{l+1} is a Gegenbauer polynomial. Now, as before, we shall replace $\exp[-\theta(s,\tau_1,\tau_2)]$ by $\xi(s,\tau_1,\tau_2)$ of Eq. (2.7). With the input potential Eq. (3.2), the kernel in Eq. (3.5) is then a sum of factorized terms. We shall discuss this case in Sec. V. As a first approximation here, we take only the first term of the sum in Eq. (3.6).[10] This is not unreasonable since, as we have realized above [Eq. (2.9)], $\xi(s,\tau_1,\tau_2)$ is a small quantity throughout the range of integration. Thus

$$\mathrm{Tr}K_l=\frac{m^2R(t)B(l+1,\frac{1}{2})}{16\pi^4}\int_{-\infty}^{0}d\tau\int_{-1}^{+1}\frac{dz(1-z^2)^{l+1/2}}{(\mu^2-\tau-\frac{1}{4}t)^2-\tau tz^2}\left(\frac{-m^2\tau}{(m^2-\tau)^2}\right)^{l+1} \tag{3.7}$$

$$=\frac{(m^2)^{l+2}R(t)}{16\pi^3(l+1)}\int_0^{\infty}du\frac{u^{l+1}}{(m^2+u)^{2l+2}}\frac{1}{(\mu^2+u+\zeta)^2}F\left(1,\tfrac{1}{2},l+2,\frac{4u\zeta}{(\mu^2+u+\zeta)^2}\right), \tag{3.8}$$

where we have used the notation $u=-\tau$ and $\zeta=-\frac{1}{4}t$ for convenience. Now observe that, for a given $\zeta>0$, the expression $(4u\zeta)/(\mu^2+u+\zeta)^2$ is always less than or equal to unity throughout the range of integration

$$\left.\frac{4u\zeta}{(\mu^2+u+\zeta)^2}\right|_{u=\mu^2+\zeta}^{\max}=\frac{\zeta}{\mu^2+\zeta}\begin{cases}<1 & \text{for } \mu^2\neq 0\\ =1 & \text{for } \mu^2=0.\end{cases} \tag{3.9}$$

Thus, the expansion of F as a hypergeometric series in powers of $(4u\zeta)/(\mu^2+u+\zeta)^2$ always stays within the radius of convergence of the series for $\mathrm{Re}\,l>-2$. After this expansion has been made, the series can be integrated term by term, each term being expressed as a hypergeometric function. Thus we get a series of hypergeometric functions with coefficients $(\zeta/m^2)^n$. The first two terms are as follows:

$$\mathrm{Tr}K_l=\frac{R(t)}{16\pi^3(l+1)}\left[B(l+2,l+2)F\left(2,l+2,2l+4,1-\frac{\mu^2+\zeta}{m^2}\right)\right.$$
$$\left.+\frac{4}{2(l+2)}\left(\frac{\zeta}{m^2}\right)B(l+1,l+3)F\left(4,l+1,2l+4,1-\frac{\mu^2+\zeta}{m^2}\right)+O((\zeta/m^2)^2F)\right]. \tag{3.10}$$

The next step is to transform[11] $F(a,b,c,1-x)$ into $F(a',b',c',x)$ and then to express $F(a',b',c',x)$ as a hypergeometric series in powers of $x\equiv(\mu^2+\zeta)/(m^2)$ [since we shall be interested only in the small-t region where $(\mu^2+\zeta)/(m^2)\leq 1$]. After this manipulation, we obtain the eigenvalue condition

$$
\begin{aligned}
1 &= \mathrm{Tr}K_l \\
&= \frac{R(t)}{16\pi^3}\left(\frac{B(l,l)}{2(2l+1)}\left[1+\frac{2(l+2)}{-l+1}\left(\frac{\mu^2+\zeta}{m^2}\right)+\frac{2(l+2)}{-l+1}\frac{3(l+3)}{-l+2}\frac{1}{2}\left(\frac{\mu^2+\zeta}{m^2}\right)^2+\cdots\right]\right. \\
&\quad -\frac{\pi}{\sin\pi l}\left(\frac{\mu^2+\zeta}{m^2}\right)^l\left[1+\frac{(2l+2)(l+2)}{l+1}\left(\frac{\mu^2+\zeta}{m^2}\right)+\frac{(2l+2)(l+2)}{l+1}\frac{(2l+3)(l+3)}{l+2}\frac{1}{2}\left(\frac{\mu^2+\zeta}{m^2}\right)^2+\cdots\right] \\
&\quad +\frac{4}{2(l+2)}\left(\frac{\zeta}{m^2}\right)\left\{-B(l,l)\frac{l}{-l+1}\left[\frac{1}{l+1}+\frac{4}{-l+2}\left(\frac{\mu^2+\zeta}{m^2}\right)+\cdots\right]\right. \\
&\quad \left.\left.+\frac{l(l+2)}{6}\frac{\pi}{\sin\pi l}\left(\frac{\mu^2+\zeta}{m^2}\right)^{l-1}\left[1+\frac{2l(l+3)}{l}\left(\frac{\mu^2+\zeta}{m^2}\right)+\cdots\right]\right\}+O((\zeta/m^2)^2F)\right). \qquad (3.11)
\end{aligned}
$$

Notice that in Eq. (3.11), the radius of convergence of the series is controlled by m^2. Therefore, for $t\neq 0$, even if $\mu^2\to 0$, the solution $l(t)$ of Eq. (3.11) remains finite. If, instead of the procedure following Eq. (3.8), a direct expansion of the nonforward propagator were made in the form

$$
\frac{1}{(\mu^2-\tau-\frac{1}{4}t)^2-\tau t z^2}=\frac{1}{(\mu^2-\tau)^2}\left(1+\frac{1}{2}\frac{t}{(\mu^2-\tau)}-\frac{t\tau z^2}{(\mu^2-\tau)^2}+\cdots\right), \qquad (3.12)
$$

one would obtain a series representation of $\mathrm{Tr}K_l$ with a radius of convergence that is essentially controlled by μ^2. Thus such a procedure would suggest that $\mathrm{Tr}K_l\to\infty$ for $\mu^2\to 0$ and $l<1$, even though the corresponding integral representation of $\mathrm{Tr}K_l$ is actually finite in this limit.[6,8]

The slopes of the trajectories can easily be computed from Eq. (3.11) by the formula

$$
\frac{dl}{dt}=-\frac{\partial\,\mathrm{Tr}K_l}{\partial t}\Big/\frac{\partial\,\mathrm{Tr}K_l}{\partial l}.
$$

Thus

$$
\left.\frac{d\alpha}{dt}\right|_{t=0}=\frac{1}{Y(0)}\left[\frac{1}{4m^2}X(0)-\frac{16\pi^3}{R(0)}\left(\frac{2m^2}{\Delta(m^2,\mu^2,\mu^2)}\right)P_L'(1)\right], \qquad (3.13)
$$

in which α satisfies Eq. (3.11) and

$$
X(0)=\left(\frac{\partial}{\partial\zeta}\frac{16\pi^3}{R(t)}\mathrm{Tr}K_l\right)_{l=\alpha(0),\,\zeta=0} \qquad (3.14)
$$

$$
\begin{aligned}
&=\frac{B(\alpha,\alpha)(\alpha+2)}{(-\alpha+1)(2\alpha+1)}\left[1+\frac{3(\alpha+3)}{(-\alpha+2)}\left(\frac{\mu^2}{m^2}\right)+\cdots\right]-\frac{\pi}{\sin\pi\alpha}\left(\frac{\mu^2}{m^2}\right)^{\alpha-1}\left[\alpha+2(\alpha+1)(\alpha+2)\left(\frac{\mu^2}{m^2}\right)+\cdots\right] \\
&\quad -\frac{2\alpha B(\alpha,\alpha)}{(-\alpha+1)(\alpha+1)(\alpha+2)}\left[1+\frac{4(\alpha+1)}{(-\alpha+2)}\left(\frac{\mu^2}{m^2}\right)+\cdots\right]+\frac{\pi}{\sin\pi\alpha}\frac{\alpha}{3}\left(\frac{\mu^2}{m^2}\right)^{\alpha-1}\left[1+2(\alpha+3)\left(\frac{\mu^2}{m^2}\right)+\cdots\right] \qquad (3.15)
\end{aligned}
$$

$$
\underset{\alpha=1}{=}\left[\frac{43}{18}+\frac{2}{3}\ln\left(\frac{\mu^2}{m^2}\right)\right]+\left[\frac{169}{9}+\frac{28}{3}\ln\left(\frac{\mu^2}{m^2}\right)\right]\left(\frac{\mu^2}{m^2}\right)+\cdots, \qquad (3.16)
$$

$$
Y(0)=\left(\frac{\partial}{\partial l}\frac{16\pi^3}{R(t)}\mathrm{Tr}K_l\right)_{l=\alpha(0),\,\zeta=0} \qquad (3.17)
$$

$$
\begin{aligned}
&=\left(\frac{\dot B(\alpha,\alpha)}{2(2\alpha+1)}-\frac{B(\alpha,\alpha)}{(2\alpha+1)^2}\right)+\left(\frac{\dot B(\alpha,\alpha)(\alpha+2)}{(-\alpha+1)(2\alpha+1)}-\frac{3B(\alpha,\alpha)}{(-\alpha+1)(2\alpha+1)^2}+\frac{B(\alpha,\alpha)(\alpha+2)}{(-\alpha+1)^2(2\alpha+1)}\right)\left(\frac{\mu^2}{m^2}\right)+\cdots \\
&\quad +\left[\frac{-\pi}{\sin\pi\alpha}\left(\frac{\mu^2}{m^2}\right)^{\alpha}\ln\left(\frac{\mu^2}{m^2}\right)+\left(\frac{\pi}{\sin\pi\alpha}\right)^2(\cos\pi\alpha)\left(\frac{\mu^2}{m^2}\right)^{\alpha}\right]\left[1+2(\alpha+2)\left(\frac{\mu^2}{m^2}\right)+\cdots\right]-2\frac{\pi}{\sin\pi\alpha}\left(\frac{\mu^2}{m^2}\right)^{\alpha+1}+\cdots \qquad (3.18)
\end{aligned}
$$

$$
\underset{\alpha=1}{=}-\frac{4}{9}-\frac{1}{2}\left[\frac{67}{9}-\frac{1}{3}\pi^2-\ln^2\left(\frac{\mu^2}{m^2}\right)\right]\left(\frac{\mu^2}{m^2}\right)-\cdots. \qquad (3.19)
$$

In Eq. (3.18), $\dot B(\alpha,\alpha)=2B(\alpha,\alpha)[\Psi(\alpha)-\Psi(2\alpha)]$. From these relations one sees immediately that owing to the presence of the factor $[(\mu^2)/(m^2)]^{\alpha-1}$ in $X(0)$, $d\alpha/dt|_{t=0}\to\infty$ when $\mu^2\to 0$ and $\alpha\leq 1$. Alternatively one can see this from the derivative of the integral representation of $\mathrm{Tr}K_l$ in Eq. (3.8): The integral $(\partial/\partial\zeta)\,\mathrm{Tr}K_l$ diverges at the lower end of integration when $\mu^2=0$ and $\zeta=0$. By taking $\mu^2\to 0$ we have moved the threshold from $t\doteq 4\mu^2>0$ to $t=0$.

We have also

$$A_l(\tau_1, z_1, \tau_2, z_2; t) = \frac{B(l+1, \frac{1}{2})[(1-z_1^2)(1-z_2^2)]^{(l+1)/2} R(t)}{1 - \mathrm{Tr} K_t} \left(\frac{(-m^2\tau_1)^{1/2}(-m^2\tau_2)^{1/2}}{(m^2-\tau_1)(m^2-\tau_2)} \right)^{l+1}, \tag{3.20}$$

$$A(s, \tau_1, \tau_2; t) \underset{s\to\infty}{\sim} 16\pi^3 \beta_{\alpha(t)}(t) \left(\frac{m^2}{m^2-\tau_1} \right)^{\alpha(t)+1} \left(\frac{m^2}{m^2-\tau_2} \right)^{\alpha(t)+1} \left(\frac{s}{m^2} \right)^{\alpha(t)}, \tag{3.21}$$

where, as before, $\beta_{\alpha(t)}(t) = -[Y(t)]^{-1}$.

Notice that when t (i.e., ζ) goes to zero, Eq. (3.21) coincides with Eq. (2.16). That is, in the forward limit, the leading member of the family of Regge poles ($l = \alpha - n$, $n = 0, 1, 2, \ldots$) and the corresponding Toller pole ($\lambda = \alpha$) are the same, as far as the high-energy behavior of the full amplitude is concerned. This result is true in general and does not depend on the approximation we have made. On the other hand, from Eqs. (3.20) and (2.11) we see that $A_l \to_{t\to 0} A_\lambda$ apart from the function $B(l+1, \frac{1}{2})$ and a factor with dependence on z_1 and z_2; however, this result follows only from the fact that we have discarded all the daughters ($l = \alpha - 1, \alpha - 2, \ldots$) in A_l,[9] owing to the approximation made after Eq. (3.6).

IV. EXACT NUMERICAL SOLUTION AND COMPARISON WITH APPROXIMATE SOLUTIONS

We have also solved Eqs. (2.5) and (3.5) numerically, using the method described by Wyld[12] to find the leading pole and its residue. We have considered the two cases $\mu^2 = 0$ and $\mu^2 = m_\pi^2$ (i.e., $\mu^2/m^2 = \frac{1}{30}$) for a kernel consisting of a sharp resonance of mass squared $m^2 = m_\rho^2 = 0.585\ \mathrm{GeV}^2$. The quantity R is treated as a variable parameter.

In Fig. 2 we show the numerical solution for the intercept of the leading pole when $\mu^2 = 0$. It should be noted that the method of numerical solution is not precise in this zero-μ limit: the error in α might be as high as ± 0.1. The value of $\alpha(0)$ calculated from Eq. (3.11) with $\mu^2 = 0$ and $\zeta = 0$ is also plotted; it differs from the numerical solution by about 6% when $\alpha = 1$. For the sake of comparison we have also plotted the values of $\alpha(0)$ calculated in the trace approximation[2]

$$1 = \frac{R(0)}{16\pi^3} \frac{2}{\alpha(\alpha+1)(\alpha+2)} \tag{4.1}$$

(dashed line), and the approximate solution of Ref. 5

$$1 = \frac{R(0)}{16\pi^3} \frac{1}{\alpha(\alpha+1)} \tag{4.2}$$

(dotted line), which is also the expression obtained in Ref. 6.

Figure 3 shows the numerical solution for $\alpha(0)$ when $(\mu^2)/(m^2) = \frac{1}{30}$, together with the value of $\alpha(0)$ calculated from Eq. (3.11) to first order in $(\mu^2)/(m^2)$.

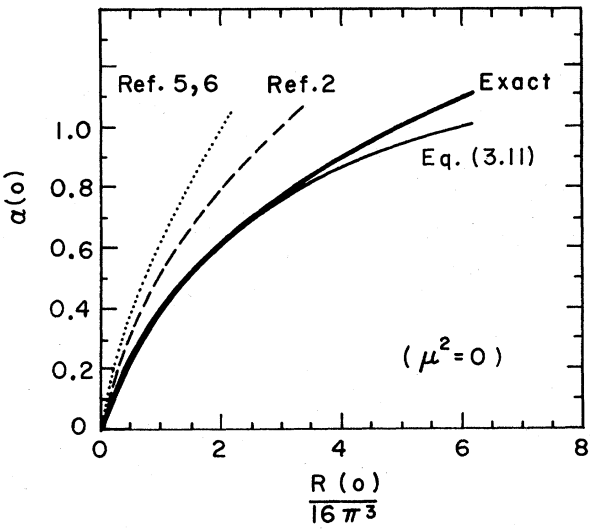

FIG. 2. Solutions for the intercept of the leading pole when $\mu^2 = 0$.

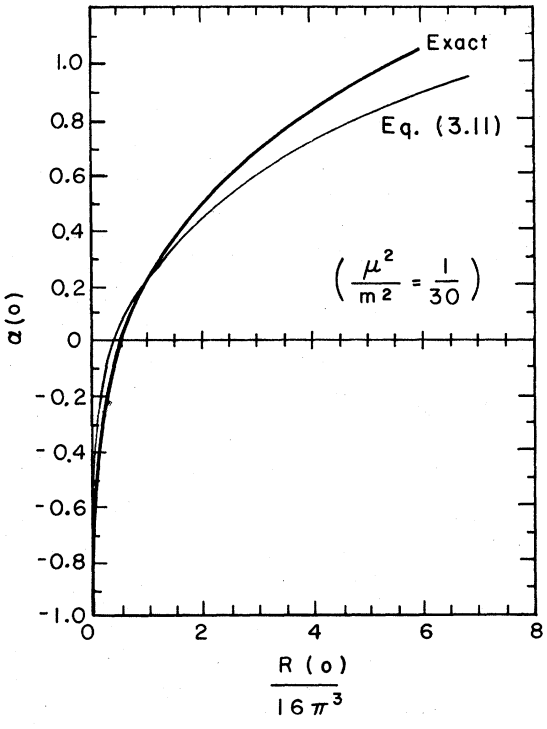

FIG. 3. Solutions for the intercept of the leading pole when $\mu^2 = m_\pi^2$.

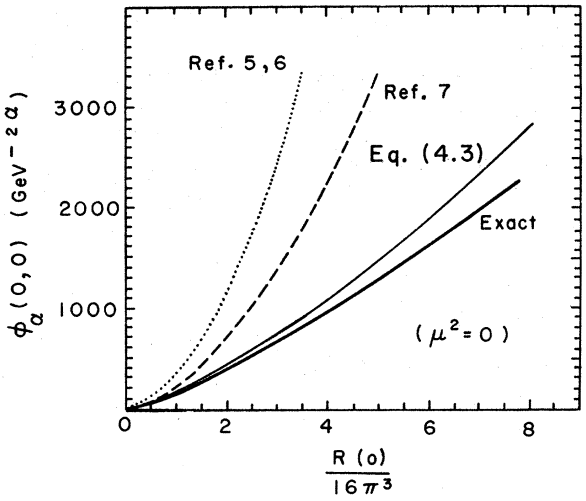

FIG. 4. Solutions for the residue of the leading pole when $\mu^2=0$.

Figure 4 shows the numerical solution for the residue of the leading pole defined in Eq. (2.19) when $\mu^2=0$. In this figure we have also plotted our approximate solution from Eq. (2.18),

$$\phi_\alpha(0,0)\sim 16\pi^3\beta_\alpha\frac{1}{(m^2)^\alpha}, \tag{4.3}$$

where $\beta_\alpha(0)=-[Y(0)]^{-1}$ with $\mu^2=0$ in Eq. (3.17). Again we also show the value of $\phi_\alpha(0,0)$ calculated from Ref. 7 (dashed line) and from the eigenvalue condition [our Eq. (4.2)] of Refs. 5 and 6 (dotted line). For $[R(0)]/(16\pi^3)=4$, say, Eq. (4.3) misses the exact solution by about 10%, whereas the other approximate solutions miss by more than 100%.

In Fig. 5 we show the numerical solution for

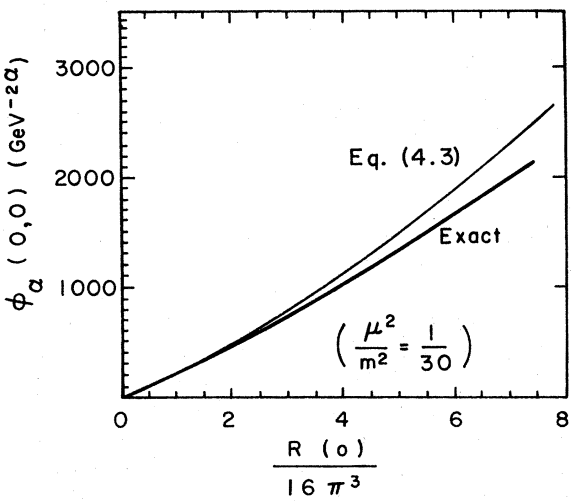

FIG. 5. Solutions for the residue of the leading pole when $\mu^2=m_\pi^2$.

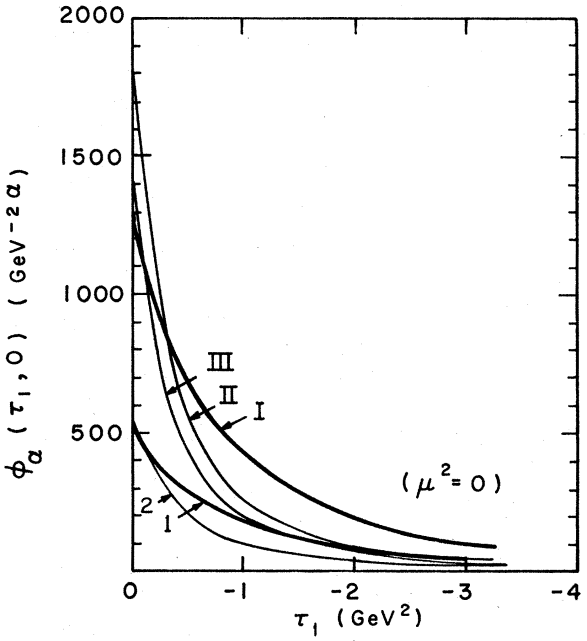

FIG. 6. Off-shell dependence of the residue of the leading pole when $\mu^2=0$. The exact numerical solutions are shown in heavy lines, whereas $\phi_\alpha(\tau_1,0)$ calculated from Eq. (4) are shown in light lines. Curve I: $\alpha(0)=1$, $R(0)/16\pi^3=4.95$. Curve II: $\alpha(0)=1$, $R(0)/16\pi^3=6$. Curve III: $\alpha(0)=0.94$, $R(0)/16\pi^3=4.95$. Curves 1 and 2: $\alpha(0)=0.7$, $R(0)/16\pi^3\approx 2.5$.

$\phi_\alpha(0,0)$ when $(\mu^2)/(m^2)=\frac{1}{30}$. The approximate solution given by Eq. (4.3) with $\beta_\alpha=-[Y(0)]^{-1}$ is also shown to first order in $(\mu^2)/(m^2)$.

Figure 6 shows the off-shell dependence of the residue of the leading pole when $\mu^2=0$. From Eq. (2.16), we have

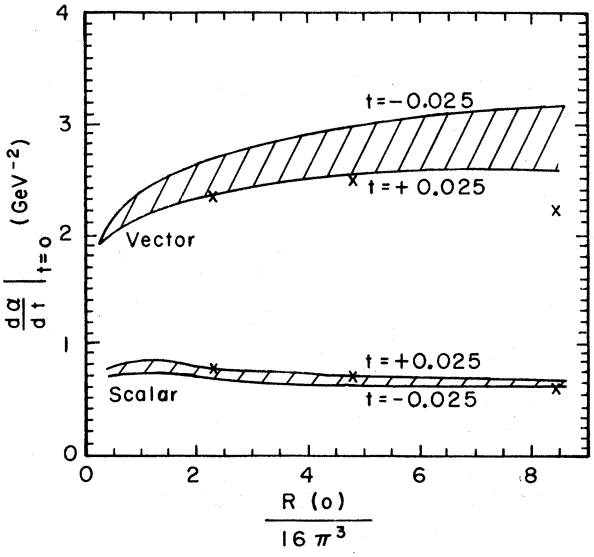

FIG. 7. Slope of the leading pole at $t=0$.

$$\phi_\alpha(\tau_1, 0) = \phi_\alpha(0, 0)\left(\frac{m^2}{m^2 - \tau_1}\right)^{\alpha+1}. \tag{4.4}$$

It is seen that the approximate solutions are "more peripheral" than the exact ones. This is not surprising since we have replaced the original kernel by the one which is more peripheral [cf., Eqs. (2.6) and (2.7)].

Finally, in Fig. 7 we show the slope of the leading pole at $t=0$, when the μ-μ resonance is (i) a scalar and (ii) a vector. The numerical solution for $t=0$ lies somewhere within the shaded area. We have also computed the values of the slope at $t=0$ according to Eq. (3.13) up to order $[(\mu^2)/(m^2)]^2$ at three different values of $R(0)$ corresponding to $\alpha(0)=0.5$, 0.8, and 1.0.[13] They are shown as x's in the figure.

V. GENERALIZATIONS

Let us consider briefly the case of a kernel consisting of a finite sum of factorized (and symmetric) terms. The sum may arise either from the input of many resonances in Eq. (2.10) or from taking more terms in the series of Eq. (3.6). For example, if we put

$$V(s, \mu^2, \mu^2) = \sum_{i=1}^{n} m_i^2 R_i \delta(s - m_i^2),$$

then we have

$$V_\lambda(\tau_1, \tau_2) = \sum_i \left[m_i R_i^{1/2}\left(\frac{m_i(-\tau_1)^{1/2}}{m_i^2 - \tau_1}\right)^{\lambda+1}\right]\left[m_i R_i^{1/2}\left(\frac{m_i(-\tau_2)^{1/2}}{m_i^2 - \tau_2}\right)^{\lambda+1}\right], \tag{5.1}$$

which is no longer factorizable in τ_1 and τ_2. The resulting equation can be solved by an algebraic method. That is, for an integral equation of the type

$$f(\tau_1, \tau_2) = V(\tau_1, \tau_2) + \int V(\tau_1, \tau') S(\tau') f(\tau', \tau_2) d\tau' \tag{5.2}$$

with

$$V(\tau_1, \tau_2) = \sum_{i=1}^{n} v_i(\tau_1) v_i(\tau_2),$$

the solution is just

$$f(\tau_1, \tau_2) = \sum_{i=1}^{n} v_i(\tau_1) v_i(\tau_2) + \sum_{i,j,k=1}^{n} v_i(\tau_1)(1 - T)_{ij}^{-1} T_{jk} v_k(\tau_2), \tag{5.3}$$

where

$$T_{ij} = T_{ji} = \int v_i(\tau) S(\tau) v_j(\tau) d\tau . \tag{5.4}$$

For the case $n=2$, for example, the solution is

$$f(\tau_1, \tau_2) = [(1 - T_{22}) v_1(\tau_1) v_1(\tau_2) + (1 - T_{11}) v_2(\tau_1) v_2(\tau_2) + T_{12} v_1(\tau_1) v_2(\tau_2) + T_{21} v_2(\tau_1) v_1(\tau_2)][(1 - T_{11})(1 - T_{22}) - T_{12} T_{21}]^{-1}, \tag{5.5}$$

which is similar to the solution to a coupled-channel problem.

VI. DISCUSSION AND CONCLUSION

From the explicit approximate solution, Eqs. (2.16), (3.11), and (3.13)–(3.21), we see the following characteristics:

(1) The leading behaviors of the trajectory and residue do not depend on the external mass μ^2; in fact, the full expressions for them remain finite in the limit $\mu^2 \to 0$ (but not for the slope at $t=0$ for $\alpha \leqslant 1$).

(2) The mass m^2 plays the role of the "scale parameter" in the factor $[(s)/(m^2)]^\alpha$ as well as in the slope formula Eq. (3.13); this scale parameter is usually asserted to be about 1 GeV^2 in Regge phenomenology. And, apart from the masses μ^2 and m^2, the residue is completely determined by the location of the pole $\alpha(t)$. In the Veneziano model, the situation is similar to that mentioned in (2) above, in that it is the reciprocal of the slope of the trajectories which serves as the scale parameter. But in that model there is an over-all factor in the residues (the constant usually denoted by β) which is not determined by the theory itself.

From the numerical solution (as well as from

the approximate solution), we see that the leading-pole position $\alpha(0)$ and the residue ϕ_α display monotonic behavior as a function of the kernel strength, which is characterized by $R(0)/16\pi^3$. As we have mentioned in Sec. II, the factorizable expression (2.7) we used is actually a lower bound to the original kernel (2.6), whereas the approximate solutions obtained by various authors[5-8] are based on some upper-bound factorizable expressions. It can be shown[14] that, for $\alpha(0)$, the approximate value obtained here is a lower bound to the exact one, while other approximate values[5-8] are its upper bounds.[15]

Let us now turn to the question of the uniqueness of our approximation scheme. As we have understood, there exist a lot of factorizable forms similar to the particular one given in Eq. (3.7). Even the conditions that we imposed in Eqs. (2.8) and (2.22) do not seem to determine $\xi(s, \tau_1, \tau_2)$ uniquely. However, if we multiply Eq. (2.7) by a factor $\gamma(s, \tau_1)\gamma(s, \tau_2)$ in which we require

$$\gamma(m^2, \tau_1)\gamma(m^2, \tau_2) = 1$$

when either τ_1 or τ_2 goes to zero (i.e., that

$$\xi(m^2, \tau_1, \tau_2)\gamma(m^2, \tau_1)\gamma(m^2, \tau_2)$$

matches $\exp[-\theta(s, \tau_1, \tau_2)]$ along the line $\tau_1 = 0$ ($\tau_2 = 0$) for all values of τ_2 (τ_1) in the τ_1-τ_2 plane), then it must be true that $\gamma(m^2, \tau) \equiv 1$ (apart from a sign).

On the other hand, if we only require $\gamma(m^2, 0) = 1$, then the condition in Eq. (2.22) imposes

$$\int_{-\infty}^{0} \frac{d\tau}{\tau^2} \left(\frac{-m^2\tau}{(m^2-\tau)^2}\right)^{\lambda+1} [\gamma^2(m^2, \tau) - \gamma(m^2, \tau)] = 0. \quad (6.1)$$

Of course $\gamma(m^2, \tau) \equiv 1$ (the original proposal) fulfills this requirement. There do exist, however, non-null functions which are orthogonal to

$$(1/\tau^2)[(-m^2\tau)/(m^2-\tau)^2]^{\lambda+1};$$

and thus one may be able to choose a suitable $\gamma(m^2, \tau)$ to match the high-τ behavior of $\exp[-\theta(s, \tau_1, \tau_2)]$. We shall not investigate this possibility further here. It suffices to say that Eq. (2.7) seems to be the simplest choice and produces a solution with reasonable analytic properties and in fairly good numerical agreement with the exact solution. We believe that such a solution will be useful in the semiquantitative study of the general physical output of the multiperipheral model, as well as in the Pomeranchukon perturbation theory.[3]

ACKNOWLEDGMENTS

We thank Dr. S. S. Shei for numerous very helpful discussions during the course of this work, and we thank Professor G. F. Chew for invaluable advice and encouragement.

---

*Work supported by the U. S. Atomic Energy Commission.

†Present address: Cavendish Laboratory, Cambridge, England.

[1] L. Bertocchi, S. Fubini, and M. Tonin, Nuovo Cimento 25, 626 (1962); D. Amati, A. Stanghellini, and S. Fubini, *ibid.* 26, 896 (1962).

[2] G. F. Chew, T. Rogers, and D. Snider, Phys. Rev. D 2, 765 (1970).

[3] H. D. I. Abarbanel, G. F. Chew, M. L. Goldberger, and L. M. Saunders, Ann. Phys. (N.Y.) (to be published), and references therein.

[4] When this work was almost completed, one of us (B.R.W.) received from Professor M. L. Goldberger a portion of his Varenna lecture notes in which a similar approximation has also been made for the kernel.

[5] In the second paper of Ref. 1.

[6] D. Silverman and P. D. Ting, University of California, San Diego Report No. UCSD-10P10-82, 1971 (unpublished).

[7] H. D. I. Abarbanel, G. F. Chew, M. L. Goldberger, and L. M. Saunders, Phys. Rev. Letters 25, 1735 (1970).

[8] J. Dash, Cambridge University Reports No. DAMTP 71/12, 1971 (unpublished), and DAMTP 71/19, 1971 (unpublished).

[9] L. M. Saunders, O. H. N. Saxton, and C.-I Tan, Phys. Rev. D 3, 1005 (1971).

[10] It can be shown, from Eq. (5.3) below and the properties of Gegenbauer polynomials, that higher terms in Eq. (3.6) affect the trajectories determined by Eq. (3.7) only to the order t^2 and higher. A similar conclusion was obtained by V. Chung and D. Snider [Phys. Rev. 162, 1639 (1967)], and M. L. Goldberger (private communication to G. F. Chew).

[11] See, for example, W. Magnus, F. Oberhettinger, and R. P. Soni, *Die Grundlehren der Mathematischen Wissenschaften in Einzeldarstellungen*, edited by J. L. Doob (Springer, New York, 1966), Vol. 52. The formula we needed is

$$F(a,b,c,1-x) = \frac{\Gamma(c)\Gamma(c-a-b)}{\Gamma(c-b)\Gamma(c-a)} F(a,b,a+b-c+1,x) + x^{c-a-b} \frac{\Gamma(c)\Gamma(a+b-c)}{\Gamma(a)\Gamma(b)} \times F(c-a,c-b,c-a-b+1,x),$$

for $|\arg x| < \pi$. When $c-a-b = \pm 0, \pm 1, \pm 2, \ldots$, this expression is still valid but we must pass to the limit with care, e.g.,

$$F(a,b,a+b+k,1-x) = \frac{\Gamma(k)\Gamma(a+b+k)}{\Gamma(a+k)\Gamma(b+k)} \sum_{n=0}^{k-1} \frac{\Gamma(a+n)\Gamma(b+n)}{\Gamma(a)\Gamma(b)} \frac{\Gamma(1-k)}{\Gamma(1-k+n)} \frac{x^n}{n!} - \frac{\Gamma(a+b+k)}{\Gamma(a)\Gamma(b)} x^k \sum_{n=0}^{\infty} \frac{\Gamma(a+k+n)\Gamma(b+k+n)}{\Gamma(a+k)\Gamma(b+k)} \frac{x^n}{n!(k+n)!} \times [\ln x - \Psi(n+1) + \Psi(a+k+n) + \Psi(b+k+n) - \Psi(1+k+n)]$$

for $|\arg x|<x$, $|x|<1$, $k=1,2,3,\ldots$. This gives, for example, Eq. (3.11) below when $\zeta=0$ and $l\to 1$,

$$1=\frac{R(0)}{16\pi^3}\left[\frac{1}{6}+\left(\ln\frac{\mu^2}{m^2}+\frac{7}{3}\right)\left(\frac{\mu^2}{m^2}\right)+6\left(\ln\frac{\mu^2}{m^2}+\frac{17}{12}\right)\left(\frac{\mu^2}{m^2}\right)^2+\cdots\right].$$

[12]H. W. Wyld, Jr., Phys. Rev. D 3, 3090 (1971).

[13]We computed the slope to order $[(\mu^2)/(m^2)]^2$ because the series X in Eq. (3.15) and Y in Eq. (3.18) converge less rapidly than that in Eq. (3.11). Although the $O([(\mu^2)/(m^2)]^2)$ terms are in magnitude only about 15% of the $O(1)+O((\mu^2)/(m^2))$ terms, they contribute with opposite signs to X and Y, making the quotient X/Y change by about 30%.

[14]G. Tiktopoulos and S. B. Treiman, Phys. Rev. 137, B1597 (1965).

[15]Our approximate solution shown in Fig. 3 lies slightly above the exact solution for $\alpha(0)\lesssim\frac{1}{3}$. This is due to the fact that we have computed $\alpha(0)$ from Eq. (3.11) only up to first order in $(\mu^2)/(m^2)$. Inclusion of higher-order $(\mu^2)/(m^2)$ terms will make it lie below the exact solution in that region also.

PHYSICAL REVIEW D VOLUME 5, NUMBER 4 15 FEBRUARY 1972

Feynman-Diagram Models of Fermion Regge-Pole Conspiracies*

David C. Robertson
Institute of Theoretical Science, University of Oregon, Eugene, Oregon 97403
(Received 9 August 1971)

A Feynman-diagram model of spin-J fermion Regge poles is developed for meson-nucleon scattering and is used to study the conspiracies arising from two types of Lorentz-invariant couplings. For a completely symmetric coupling, the model automatically leads to a conspiracy relation ($M=\frac{1}{2}$) between two leading trajectories of opposite parity which are Mac-Dowell partners. The second type of coupling, which is antisymmetric in two indices, leads to an $M=\frac{3}{2}$ conspiracy relation between four leading trajectories. At high energies, the $M=\frac{1}{2}$ conspiracy favors the scattering of spin-1 mesons with zero helicity in both initial and final states while the $M=\frac{3}{2}$ conspiracy favors mesons of helicity ±1. Since the $M=\frac{3}{2}$ trajectory chooses nonsense coupling at $J=\frac{1}{2}$, the lowest spin of a particle on the trajectory is $\frac{3}{2}$.

I. INTRODUCTION

In Regge-pole theory Feynman-diagram models have proven to be a useful tool in studying the analytic structure of the scattering amplitudes. They provide a convenient method of coupling a Regge pole to the external particles so that the basic notions of analyticity are satisfied. In these models, the introduction of daughter and conspirator Regge trajectories to restore analyticity to the scattering amplitude[1] arises in a natural way. The numerator of the high-spin off-mass-shell Feynman propagators carries lower-spin components which combine to cancel the singular parts of the spin-J projection operators. Models of this type were first studied by Van Hove and Durand.[2] They have been used to study fermion and boson daughter trajectories[3,4] and have been extended to incorporate boson conspiracies.[5,6]

This paper studies fermion conspiracies within the framework of the Feynman-diagram models. It will be shown that the amplitude for Regge-pole exchange automatically contains the necessary conspiring Regge trajectories to maintain analyticity. Since we are studying conspiring Regge trajectories, the masses of the external particles will be taken to be equal, so that the daughter trajectories which arise from unequal external masses will decouple from the scattering amplitude. Signature will be ignored since it can be trivially included at the end of the calculation.

Within the framework of the one-particle-exchange (OPE) model of Van Hove and Durand, we will see that the conspiracy relations for π-N scattering are automatically satisfied by Mac-Dowell-symmetric[7] baryon trajectories. We will then look at the meson-baryon scattering in a more general four-point coupling model in which the coupling is via Lorentz-invariant tensors. For ρ-N scattering this leads to more complicated conspiracy relations among the leading Regge trajectories and makes definite predictions about the ρ's density matrix. These predictions depend only on the form of the Lorentz-invariant couplings and should be independent of the dynamical details of the model.

The angular momentum part of the coupling between the external particles and the Regge pole is obtained by use of Lorentz-invariant tensors. The dynamical part of the coupling is taken as a con-